J. Marine Sci. Appl. (2014) 13: 200-205
DOI: 10.1007/s11804-014-1251-0

Forced Axial and Torsional Vibrations of a Shaft Line Using the Transfer Matrix Method Related to Solution Coefficients

Kandouci Chahr-Eddine* **and Adjal Yassine**

Department of Maritime Engineering, University of Sciences and Technology USTO-MB, Oran 31000, Algeria

Abstract: This present paper deals with a mathematical description of linear axial and torsional vibrations. The normal and tangential stress tensor components produced by axial-torsional deformations and vibrations in the propeller and intermediate shafts, under the influence of propeller-induced static and variable hydrodynamic excitations are also studied. The transfer matrix method related to the constant coefficients of differential equation solutions is used. The advantage of the latter as compared with a well-known method of transfer matrix associated with state vector is the possibility of reducing the number of multiplied matrices when adjacent shaft segments have the same material properties and diameters. The results show that there is no risk of buckling and confirm that the strength of the shaft line depends on the value of the static tangential stresses which is the most important component of the stress tensor.

Keywords: shaft line; stress tensor; vibration; axial vibration; torsional vibration; transfer matrix; constant coefficient vector

Article ID: 1671-9433(2014)02-0200-06

1 Introduction

The hydrodynamic excitations generated by the running marine propeller in a non-homogeneous hydrodynamic environment may cause significant vibrations in the line shafting system. The dominant variable components of propeller excitations usually have a pulsation equal to the first blade harmonic. Particular attention of classification society rules focus on torsional vibrations of the marine shafting system and their tangential dynamic stresses which may cause shaft failures (Bureau Veritas, 2011; Lloyd's Register, 2012). It is required that torsional vibration of the shafting system be calculated during the design stage and then measured during sea trials. On the other hand, for all main propulsion shafting systems, the shipbuilders have to ensure that axial vibration amplitudes are satisfactory throughout the speed range (Lloyd's Register, 2012). Axial vibrations are a result of propeller thrust fluctuations mainly located between the propeller and thrust bearing.

Vibration analyses of marine shafting systems have been conducted by many researchers in order to improve on a method to estimate the geometries and properties of each shafting element. The forced torsional vibration stress curves obtained from measured vibration at the free end of the propulsion shafting are compared with the results obtained from the calculation of forced vibration, by Tang *and* Brennan (2013). The results show that a highly flexible component may have a significant effect on the mode shapes. A numerical analysis of the axial vibration taking into account the couplings is compared with the measurement performed on a real ship by Murawski (2004).

The transfer matrix method relating to state vectors was introduced by Myklestad in the 1940s, and generalized by Prohl and then gradually developed by other researchers. In the field of marine shafting vibrations, Davor (1997) used this method to investigate the coupling between torsional and axial vibrations resulting from a propeller in the solid elastic shaft of merchant ocean going ships. In this aspect this method was used to evaluate the frequencies of the tail shaft transverse vibrations of ships by JIA (2008). The transfer matrix method related to state vectors is widely used for the calculation of free and forced vibrations. Consequently the difficulty lies in the high order of multiplied matrices in the case of long shaft lines. In the present study, the transfer matrix method related to solution coefficients of differential equations has been developed. This method applied to the shafting system was proposed in the works of Kolenda (1979). It has been used for calculations of forced coupled flexural vibrations (Vinh Phat, 1988) and for strength analysis of shaft lines (Kandouci, 1992).

The advantage of this method as compared with a well-known method of transfer matrix associated with state vectors is the reduction of the number of multiplied matrices in to one matrix when adjacent shaft segments have the same material properties and diameters. Normal and tangential stresses due to the static and variable hydrodynamic excitation components are also studied.

2 Physical model of the analyzed system

2.1 physical model of shafts

A physical model of the analyzed system is shown in Fig.1. It concerns shaft line parts in which the effects of propeller hydrodynamic excitations is greatest. More precisely the propeller and intermediate shafts, clamped at

Received date: 2013-11-28.
Accepted date: 2014-04-22.
***Corresponding author Email:** kan_cha31@yahoo.fr

the place of the axial thrust bearing.

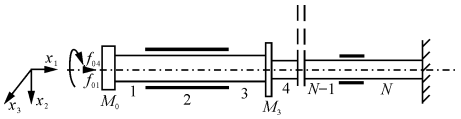

Fig.1 Physical model of the system

The shaft line material is considered to be isotropic, the propeller and the coupling flange are assumed to be discrete masses and it is supposed that the inertia central principal axis of each shaft sections coincides with the rotation axis.

$$\boldsymbol{f}_0 = [f_{01} \quad f_{04}]^{\mathrm{T}} = \{f_{0\alpha}\}$$

where, $\boldsymbol{f}_0$ is the vector of hydrodynamic propeller excitations including just the thrust and torsional moment of the propeller, $\alpha = 1$ concerns the axial force (propeller thrust), $\alpha = 4$ is the torsional moment. $\boldsymbol{M}_0 = [m_{01} \quad m_{04}]$ is the propeller inertia matrix including the added water mass, $\boldsymbol{M}_3$ is the flange coupling inertia matrix located at the end of the third shaft line segment.

We assume that the system is linear and its vibrations in a fixed local coordinate system are governed by the following differential equations:

$$\frac{\partial^2 u_{ix1}}{\partial t^2} - \left[\frac{E}{\rho}\right]_i \frac{\partial^2 u_{ix1}}{\partial x^2} = 0 \tag{1}$$

$$\frac{\partial^2 u_{ix4}}{\partial t^2} - \left[\frac{G}{\rho}\right]_i \frac{\partial^2 u_{ix4}}{\partial x^2} = 0 \tag{2}$$

where, u_{ix1} represents the axial vibration of the i-th segment in the section x, in the longitudinal direction (α = 1); u_{ix4} represents torsional vibration (α = 4); $\boldsymbol{u}_{ix} = \{u_{ix1}, u_{ix4}\}$ is the vibration vector in the section $x_{i1} = x$.

Internal force and moment $p_{ix\alpha}$ are given by the known beam theory:

$$p_{ix1} = EA_i \frac{\partial u_{ix1}}{\partial x}, \; p_{ix4} = G(I_0)_i \frac{\partial u_{ix4}}{\partial x}, \tag{3}$$

$\boldsymbol{p}_{ix} = \{p_{ix1}, p_{ix4}\}$ is the internal force vector in the section $x_{i1} = x$.

In the above Eqs. (1)-(3), E, A_i, G and $(I_0)_i$ are respectively Young's modulus, cross area section, Kirchhoff's modulus and the polar moment of inertia of the i-th shaft cross section, ρ is the density of the shaft material.

The boundary conditions at the left and right ends of the system are respectively:

$$-p_{10\alpha} + (m_{0\alpha}\ddot{u}_{10\alpha} + c_{0\alpha}\dot{u}_{10\alpha}) = f_{0\alpha} \tag{4}$$

$$u_{NL\alpha} = 0 \tag{5}$$

where $\alpha = 1, 4$, the coefficients $m_{0\alpha}$ and $c_{0\alpha}$ are respectively the elements of the propeller inertia matrix (taking into account the added water mass) and the viscous damping coefficient matrix of the water.

Corresponding stresses due to the internal force and moment $p_{i\alpha x}$ are:

$$\sigma_{1x1} = \frac{p_{ix1}}{A_i}, \; \sigma_{ix4} = \frac{p_{ix4}}{(W_0)_i} \tag{6}$$

where $(W_0)_i$ represents the torsional modulus of the i-th shaft, $\boldsymbol{\sigma}_{ix} = \{\sigma_{ix1}, \sigma_{ix4}\}$ is the stress vector in the section $x_{i1} = x$.

The hydrodynamic excitations acting on the propeller rotating at speed ω_o are expressed as:

$$f_{0\alpha} = f_{0\alpha}^{(0)} + \sum_{\nu} f_{0\alpha}^{(\nu)} \cos\left(\nu\omega_0 t + \theta_{0\alpha}^{(\nu)}\right), \quad \nu = 1, 2, \ldots \tag{7}$$

and can be written in complex form:

$$f_{0\alpha} = \sum_{\nu} f_{0\alpha}^{(\nu)} \mathrm{e}^{\mathrm{j}\nu\omega_0 t}, \; \nu = 0, 1, \ldots \tag{8}$$

where $f_{0\alpha}^{(\nu)}$ is the complex amplitude defined as:

$$f_{0\alpha}^{(\nu)} = \overline{f}_{0\alpha}^{(\nu)} \mathrm{e}^{\mathrm{i}\theta_{0\alpha}^{(\nu)}} \tag{9}$$

in which, $\overline{f}_{0\alpha}^{(\nu)}$ is the real amplitude of the ν-th component of the propeller hydrodynamic excitation, in the direction α; $\theta_{0\alpha}^{(\nu)}$ represents initial phase of the ν-th component of the hydrodynamic excitation, in the direction α; ω_0 is angular velocity of the propeller.

Vibrations, internal forces and stresses are looked for, like the real parts of the following expressions:

$$u_{ix\alpha} = \sum_{\nu} \overline{u}_{ix\alpha}^{(\nu)} \mathrm{e}^{\mathrm{j}\nu\omega_0 t} \tag{10}$$

$$p_{ix\alpha} = \sum_{\nu} \overline{p}_{ix\alpha}^{(\nu)} \mathrm{e}^{\mathrm{j}\nu\omega_0 t} \tag{11}$$

$$\sigma_{ix\alpha} = \sum_{\nu} \overline{\sigma}_{ix\alpha}^{(\nu)} \mathrm{e}^{\mathrm{j}\nu\omega_0 t} \tag{12}$$

Substituting Eq. (10) into differential Eqs. (1) and (2), we can get:

$$u_{ix} = \sum_{\nu} \overline{u}_{ix\alpha}^{(\nu)} \mathrm{e}^{\mathrm{j}\nu\omega_0 t} \tag{13}$$

$$\overline{u}_{ix}^{(\nu)} = \boldsymbol{C}_{ix}^{(\nu)} \boldsymbol{a}_i^{(\nu)} \tag{14}$$

where,

$$\boldsymbol{C}_{ix}^{(0)} = \begin{bmatrix} x & 1 & 0 & 0 \\ 0 & 0 & x & 1 \end{bmatrix}$$

$$\boldsymbol{C}_{ix}^{(\nu)} = \begin{bmatrix} \cos\left(\lambda_A^{(\nu)} x\right) & \sin\left(\lambda_A^{(\nu)} x\right) & 0 & 0 \\ 0 & 0 & \cos\left(\lambda_T^{(\nu)} x\right) & \sin\left(\lambda_T^{(\nu)} x\right) \end{bmatrix}$$

$$\lambda_A^{(\nu)} = \nu\omega(E/\rho)^{1/2}$$

$$\lambda_T^{(\nu)} = \nu\omega(G/\rho)^{1/2}$$

while

$$\boldsymbol{a}_i^{(\nu)} = \left\{a_{iq}^{(\nu)}\right\}, \quad q = 1, 2, 3, 4 \tag{15}$$

is the constant coefficient vector. The latter can be determined using the boundary conditions (4) and (5), the condition of displacement continuity and internal force equilibrium, at junctions connecting two adjacent shafts.

The vector of internal forces can be written as:

$$\boldsymbol{p}_{ix}=\sum_{\nu}\overline{\boldsymbol{p}}_{ix}^{(\nu)}\mathrm{e}^{\mathrm{j}\nu\omega_0 t} \tag{16}$$

$$\overline{\boldsymbol{p}}_{ix}^{(\nu)}=\boldsymbol{D}_{ix}^{(\nu)}a_{ix}^{(\nu)} \tag{17}$$

where,

$$\boldsymbol{D}_{ix}^{(0)}=\begin{bmatrix}-(EA)_i & 0 & 0 & 0\\ 0 & 0 & -(GI_0)_i & 0\end{bmatrix}$$

$$\boldsymbol{D}_{ix}^{(\nu)}=\left[\left(\boldsymbol{D}_{ix}^{(\nu)}\right)_1:\left(\boldsymbol{D}_{ix}^{(\nu)}\right)_2\right]$$

$$\left(\boldsymbol{D}_{ix}^{(\nu)}\right)_1=\begin{bmatrix}-\left(EA\lambda_A^{(\nu)}\right)_i\sin\left(\lambda_A^{(\nu)}x\right) & \left(EA\lambda_A^{(\nu)}\right)_i\cos\left(\lambda_A^{(\nu)}x\right)\\ 0 & 0\end{bmatrix}$$

$$\left(\boldsymbol{D}_{ix}^{(\nu)}\right)_2=\begin{bmatrix}0 & 0\\ -\left(GI_0\lambda_T^{(\nu)}\right)_i\sin\left(\lambda_T^{(\nu)}x\right) & \left(GI_0\lambda_T^{(\nu)}\right)_i\cos\left(\lambda_T^{(\nu)}x\right)\end{bmatrix}$$

2.2 an example of two adjacent shaft

For the calculation, an example of two adjacent shaft segments is illustrated in Fig 2. The axes of the coordinate system (x_{i1}, x_{i2}, x_{i3}) of the i-th segment are respectively parallel to the axes of the fixed local coordinate system (x_1, x_2, x_3) given in Fig. 1.

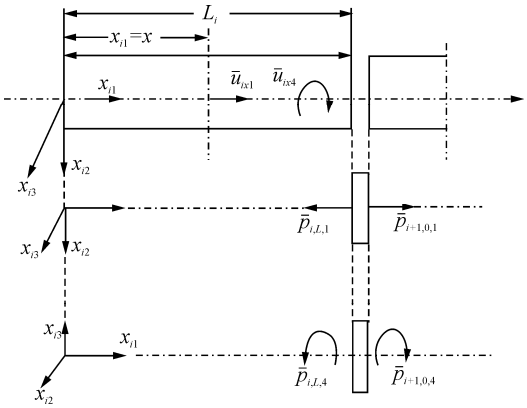

Fig. 2 Schematic illustration of two adjacent shaft segments

In Fig. 2, L_i is length of the i-th shaft segment; $p_{i,L,\alpha}$ is generalized internal force in the section $x_{i1}=x$ at the end of the i-th segment, in the direction α; $p_{i+1,0,\alpha}$ is generalized internal force in the section at the beginning of the (i+1)-th shaft segment, in the direction α; $u_{ix\alpha}$ is generalized displacement of the i-th segment, in the section $x_{i1}=x$, in the direction α.

At the junction of the two shaft segments, which have different constants of material or/and diameters, the following conditions are satisfied:

$$u_{i,L}=u_{i+1,0} \tag{18}$$

$$p_{i,L}=p_{i+1,0} \tag{19}$$

Taking into account the expressions (13), (14), (16) and (17), the conditions (18) and (19) can be written as follows:

$$\boldsymbol{C}_{i,L}^{(\nu)}\boldsymbol{a}_i^{(\nu)}=\boldsymbol{C}_{i+1,0}^{(\nu)}\boldsymbol{a}_{i+1}^{(\nu)} \tag{20}$$

$$\boldsymbol{D}_{i,L}^{(\nu)}\boldsymbol{a}_i^{(\nu)}=\boldsymbol{D}_{i+1,0}^{(\nu)}\boldsymbol{a}_{i+1}^{(\nu)} \tag{21}$$

$$\boldsymbol{a}_{i+1}^{(\nu)}=\boldsymbol{B}_i^{(\nu)}\boldsymbol{a}_i^{(\nu)} \tag{22}$$

where $\boldsymbol{B}_i^{(\nu)}$ is the transfer matrix related to the solution coefficients, calculated from expression:

$$\boldsymbol{B}_i^{(\nu)}=\begin{bmatrix}\boldsymbol{C}_{i+1,0}^{(\nu)}\\ \Delta_{i+1,0}^{(\nu)}\end{bmatrix}^{-1}\begin{bmatrix}\boldsymbol{C}_{i,L}^{(\nu)}\\ \boldsymbol{D}_{i,L}^{(\nu)}\end{bmatrix} \tag{23}$$

Using the above expressions, we obtain:

$$\boldsymbol{B}_i^{(0)}=\begin{bmatrix}\dfrac{(EA)_i}{(EA)_{i+1}} & 0 & 0 & 0\\ L_i & 1 & 0 & 0\\ 0 & 0 & \dfrac{(GI_0)_i}{(GI_0)_{i+1}} & 0\\ 0 & 0 & L_i & 1\end{bmatrix} \tag{24}$$

$$\boldsymbol{B}_i^{(\nu)}=\begin{bmatrix}\cos\left(\lambda_A^{(\nu)}L\right) & \sin\left(\lambda_A^{(\nu)}L\right) & 0 & 0\\ -e_A\sin\left(\lambda_A^{(\nu)}L\right) & e_A\cos\left(\lambda_A^{(\nu)}L\right) & 0 & 0\\ 0 & 0 & \cos\left(\lambda_T^{(\nu)}L\right) & \sin\left(\lambda_T^{(\nu)}L\right)\\ 0 & 0 & -e_T\sin\left(\lambda_T^{(\nu)}L\right) & e_T\cos\left(\lambda_T^{(\nu)}L\right)\end{bmatrix} \tag{25}$$

$$\left(e_A^{(\nu)}\right)_i=\frac{\left(EA\lambda_A^{(\nu)}\right)_i}{\left(EA\lambda_A^{(\nu)}\right)_{i+1}},\ \left(e_T^{(\nu)}\right)_i=\frac{\left(GI_0\lambda_T^{(\nu)}\right)_i}{\left(GI_0\lambda_T^{(\nu)}\right)_{i+1}} \tag{26}$$

For the $s-1$ following shaft segments, we have the relationship:

$$\boldsymbol{a}_{i+s}^{(\nu)}=\boldsymbol{B}_{i+s-1}^{(\nu)}\boldsymbol{B}_{i+s-2}^{(\nu)}\cdots\boldsymbol{B}_i^{(\nu)}a_i^{(\nu)} \tag{27}$$

For the calculation of the shaft line vibration, the number of multiplied matrices in Eq. (27) may be large, however the matrices $B_i^{(\nu)}$ present an advantageous property, when the shaft segments have the same material constants and diameter, the expression (27) is reduced to:

$$\boldsymbol{a}_{i+S}^{(\nu)}=\boldsymbol{G}_i^{(\nu)}\boldsymbol{a}_i^{(\nu)} \tag{28}$$

where the matrix $\boldsymbol{G}_i^{(\nu)}$ is obtained from the matrix $\boldsymbol{B}_i^{(\nu)}$ by setting $(e_A)_i=(e_T)_i=1$, and replacing L_i by:

$$L_i=\sum_{p=i}^{p=i+s-1}L_p \tag{29}$$

The advantage of this method does not exist with the well-known transfer matrix relating to the state vector.

In the case where the section connecting two adjacent shaft segments passes through the center of gravity of the discrete mass, the following equations are verified:

$$u_{i,L}=u_{i+1,0} \tag{30}$$

$$p_{i,L}=p_{i+1,0}-M_i\frac{\partial^2 u_{iL}}{\partial t^2} \tag{31}$$

where M_i is the inertia matrix of discrete mass located at

the end of the *i-th* shaft segment (e.g. flange coupling). The Eqs. (30) and (31) are written as follows:

$$\boldsymbol{C}_{i,L}^{(\nu)}\boldsymbol{a}_i^{(\nu)} = \boldsymbol{C}_{i+1,0}^{(\nu)}\boldsymbol{a}_{i+1}^{(\nu)} \tag{32}$$

$$\boldsymbol{D}_{i,L}^{(\nu)}\boldsymbol{a}_i^{(\nu)} = \boldsymbol{D}_{i+1,0}^{(\nu)}\boldsymbol{a}_{i+1}^{(\nu)} + (\nu\omega_0)^2\boldsymbol{M}_i\boldsymbol{C}_{i,L}^{(\nu)}\boldsymbol{a}_i^{(\nu)} \tag{33}$$

where, $\boldsymbol{M}_i = [m_i \quad J_i]$, m_i is the discrete mass concentrated at the end of the *i*-th shaft segment, J_i is the polar moment of inertia of this mass.

According to Eqs. (32) and (33), we get:

$$\boldsymbol{a}_{i+1}^{(\nu)} = \boldsymbol{R}_i^{(\nu)}\boldsymbol{a}_i^{(\nu)} \tag{34}$$

where $R_i^{(\nu)}$ is the transfer matrix through the discrete mass.

Once these transfer matrices are calculated, we determine the vectors of the solution coefficients $\boldsymbol{a}_2^{(\nu)},\boldsymbol{a}_3^{(\nu)},\ldots,\boldsymbol{a}_N^{(\nu)}$ of the vibrations from the second to the *n*-th shaft segments, as function of $\boldsymbol{a}_1^{(\nu)}$, which is the solution coefficient vector of the first shaft vibrations.

For the system as illustrated in Fig.1, we have:

$$\begin{cases} \boldsymbol{a}_2^{(\nu)} = \boldsymbol{B}_1^{(\nu)}\boldsymbol{a}_1^{(\nu)} \\ \boldsymbol{a}_3^{(\nu)} = \boldsymbol{B}_2^{(\nu)}\boldsymbol{B}_1^{(\nu)}\boldsymbol{a}_1^{(\nu)} \\ \boldsymbol{a}_4^{(\nu)} = \boldsymbol{R}_3^{(\nu)}\boldsymbol{B}_2^{(\nu)}\boldsymbol{B}_1^{(\nu)}\boldsymbol{a}_1^{(\nu)} \\ \boldsymbol{a}_5^{(\nu)} = \boldsymbol{B}_4^{(\nu)}\boldsymbol{R}_3^{(\nu)}\boldsymbol{B}_2^{(\nu)}\boldsymbol{B}_1^{(\nu)}\boldsymbol{a}_1^{(\nu)} \\ \quad\vdots \\ \boldsymbol{a}_N^{(\nu)} = \boldsymbol{B}_{N-1}^{(\nu)}\cdots\boldsymbol{B}_4^{(\nu)}\boldsymbol{R}_3^{(\nu)}\boldsymbol{B}_2^{(\nu)}\boldsymbol{B}_1^{(\nu)}\boldsymbol{a}_1^{(\nu)} \end{cases} \tag{35}$$

In the same way, the boundary conditions (4) and (5) can be written in the form:

$$\begin{cases} \boldsymbol{D}_{1,0}^{(\nu)}\boldsymbol{a}_1^{(\nu)} + \left(\mathrm{j}\nu\omega_0\boldsymbol{B}_0 - (\nu\omega_0)^2\boldsymbol{M}_0\boldsymbol{C}_{1,0}^{(\nu)}\boldsymbol{a}_1^{(\nu)}\right) = \overline{\boldsymbol{f}}_0^{(\nu)} \\ \boldsymbol{C}_{N,L}^{(\nu)}\boldsymbol{B}_{N-1}^{(\nu)}\cdots\boldsymbol{B}_5^{(\nu)}\boldsymbol{B}_4^{(\nu)}\boldsymbol{R}_3^{(\nu)}\boldsymbol{B}_2^{(\nu)}\boldsymbol{B}_1^{(\nu)}\boldsymbol{a}_1^{(\nu)} = \boldsymbol{0} \end{cases} \tag{36}$$

As a result, we obtain the constant coefficient vector of the first shaft segment

$$\boldsymbol{a}_1^{(\nu)} = \boldsymbol{H}^{(\nu)}\overline{\boldsymbol{f}}_0^{(\nu)} \tag{37}$$

where,

$$\boldsymbol{H}^{(\nu)} = \begin{bmatrix} -\boldsymbol{D}_{1,0}^{(\nu)} + \left(\mathrm{j}\nu\omega_0\boldsymbol{B}_0 - \nu^2\omega_0^2\boldsymbol{M}_0\right)\boldsymbol{C}_{1,0}^{(\nu)} \\ \boldsymbol{C}_{N,L}^{(\nu)}\boldsymbol{B}_{N-1}^{(\nu)}\cdots\boldsymbol{B}_5^{(\nu)}\boldsymbol{B}_4^{(\nu)}\boldsymbol{R}_3^{(\nu)}\boldsymbol{B}_2^{(\nu)}\boldsymbol{B}_1^{(\nu)} \end{bmatrix}^{-1} \tag{38}$$

$\boldsymbol{B}_0$ is the viscous damping coefficient matrix of the propeller vibrations.

3 Analyzed system description

As an application, a shaft marine system of a real vessel B354 with a displacement of 10 000 DWT is used (see Fig. 3). Fig.4 represents the shaft line part analyzed.

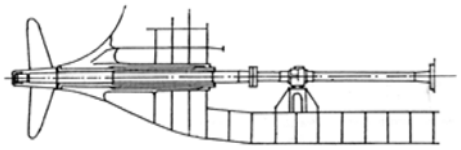

Fig. 3 Scheme of the analyzed shaft line part

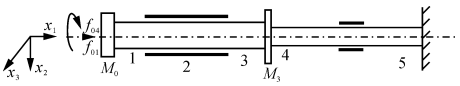

Fig. 4. Analyzed model

The parameters of the propeller and shafts are shown in Table 1 and Table 2 respectively. Young's modulus is $E = 2.1\times10^{11}$ N/m^2, Kirchhoff's modulus is $G = 0.85\times10^{11}$ N/m, and the density of the material is $\rho = 7\,680$ kg/m^3. With the flange coupling, the mass $m_3 = 1\,363.6$ kg, and the polar moment of inertia $j_3 = 164.8\ \mathrm{kg}\cdot\mathrm{m}^2$.

Table 1 Parameters of the propeller

Parameters	Value
Number of blades Z	4
Mass m_P /kg	13 500
Polar inertia moment j_P /(kg·m^2)	19 992
Nominal speed	n=117 rpm $\omega_0 = 12\ \mathrm{rad}\cdot s^{-1}$
Diameter/m	5.5

Table 2 The parameters of the shafts

number of shafts	Lengh/m	Diameter/m
1	0.84	0.560
2	3.56	0.555
3	1.55	0.565
4	1.65	0.405
5	4.80	0.405

Table 3 Propeller hydrodynamic excitations

Harmonic of blades	Parameters	Hydrodynamic excitation	
		f_{01}/N	f_{04}/(N · m)
$\nu = 0$	Value	650 700	595 600
$\nu = 4$	Amplitude	3 732	2 441
	$\theta_{0\alpha}^{(4)}$	-74°	106°
$\nu = 8$	Amplitude	7 011	44 584
	$\theta_{0\alpha}^{(8)}$	-61°	119°

According to the measurments made by the Technical Center of the Gdansk Shipyard (CTO, 1983), the first and second blade harmonics are considered. The parameters of the hydrodynamic excitations are shown in Table 3. The propeller hydrodynamic excitations have the form:

$$f_{0\alpha} = f_{0\alpha}^{(0)} + f_{0\alpha}^{(4)}\cos\left(4\omega_0 t + \theta_{0\alpha}^{(4)}\right) + f_{0\alpha}^{(8)}\cos(8\omega_0 t + \theta_{0\alpha}^{(8)})$$

4 Results of the calculations

The obtained results using a developed computer program

are given below graphically, as a function of the distance from the propeller.

Static deformations and amplitudes of the vibrations are shown in Figs. (5)-(8). Figs. (9)-(12) represent the static values and the amplitudes of the normal and tangential stresses. These are the responses of the system to the constant and variable components of the propeller hydrodynamic excitations. The jumps on the stress curves correspond to the diameter variations.

Fig. 5 shows the effect of the constant component of the thrust propeller on longitudinal deformations of the shaft line. The static tangential stresses due to the constant component of the angular momentum of the propeller are shown in Fig. 10.

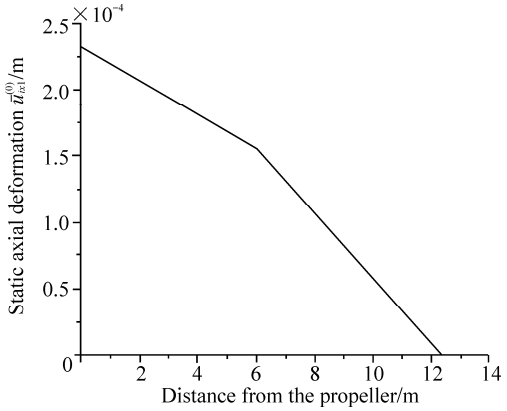

Fig. 5 Static axial deformations

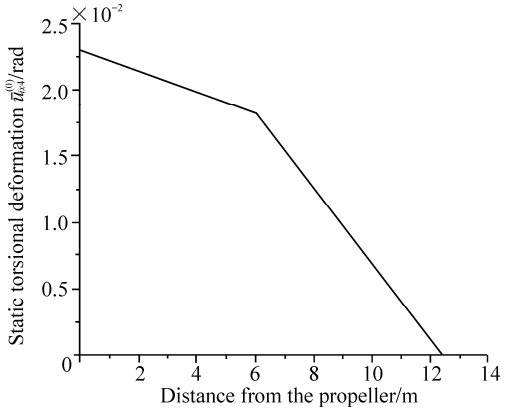

Fig. 6 Static torsional deformations

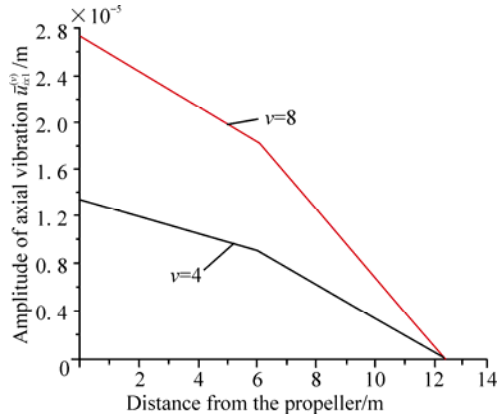

Fig. 7 Amplitudes of the axial vibrations

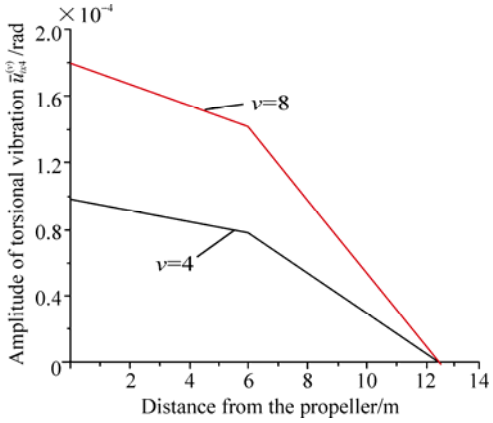

Fig. 8 Amplitudes of the torsional vibrations

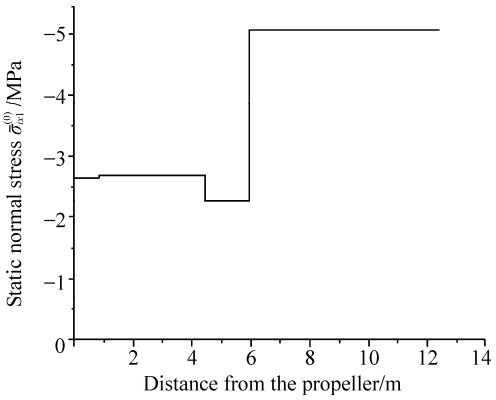

Fig. 9 Static normal stresses

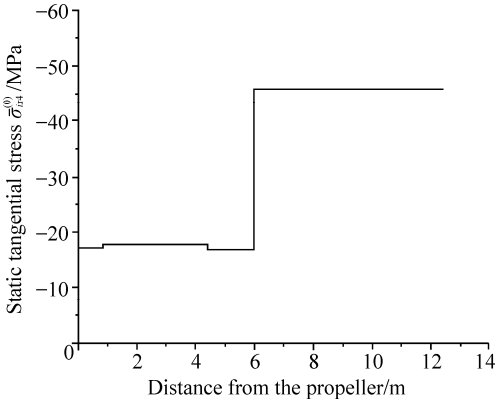

Fig.10 Static tangential stresses

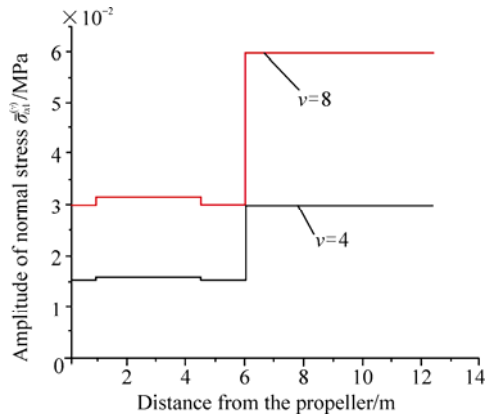

Fig. 11 Amplitudes of the normal stresses

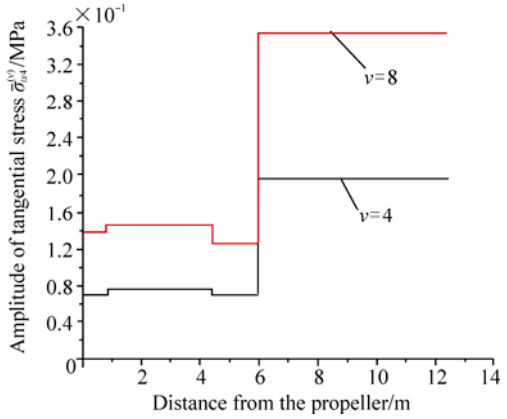

Fig. 12 Amplitudes of the tangential stresses

5 Conclusions

The results of the calculations show that, given the relatively large diameters of the different shafts, the longitudinal deformations are negligible (approximately 0.2 mm, Fig. 5), and there is no risk of buckling according to the formula of Euler. The static tangential stresses due to the static component of the propeller's moment are considerably higher than the static normal stresses due to the constant component of the propeller thrust, and are more than all the amplitudes of the variable normal and tangential stresses. The static tangential stresses due to the average angular momentum of the propeller represent the dominant component of the stress tensor. This result confirms the recommendations of the classification societies according to which, in the absence of resonance, the strength of the shaft line depends on the value of this component.

References

Bureau Veritas (2011). *BV rules for the classification of steel ships, part C: machinery, electricity, automation and fire protection*. Bureau Veritas, Neuilly-sur-Seine, France, 154-158.

CTO (1983). *Hydrodynamic forces caused by the stream after the hull*. Ship Design and Research Centre, Gdańsk, Poland. (in Polish)

Davor S (1997). *Torsional-axial coupling in the line shafting vibrations in merchant ocean going ships*. Master's thesis, Concordia University, Montreal, 10-17.

JIA XJ (2008). Analysis of the flexural vibration of ship's tail by transfer matrix method. *Journal of Marine Science and Application*, **7**(3), 179-183.

Kandouci CE (1992). *Strength Analysis of shaft line in a complex state of stress*. Ph. D. thesis, Faculty of Shipbuilding, Technical University of Gdańsk, Gdańsk, Poland. (in Polish)

Kolenda J. (1979). A more precise description of forced vibrations of shafting system with flexural asymmetric rigidity on flexible foundations. *Journal of Theoretical and Applied Mechanics*, 17(2), 105-126. (in Polish)

Lloyd's Register (2012). *LR rules and regulations for the classification of ships*. Lloyd's Register, London, UK.

Murawski L (2004). Axial vibrations of propulsion system taking in to account the couplings and the boundary conditions. *Journal of Marine Science and Technology*, **9**(4), 171-184.

Tang B, Brennan MJ (2013). On the influence of the mode shapes of marine propulsion shafting system on the prediction of torsional stresses. *Journal of Marine Science and Technology*, **21**(2), 209-214.

Vinh Phat N (1988). *Analysis of transverse vibrations of shat line taking into account the flexibility of the bearing support*. Ph. D. thesis, Institute of Shipbuilding, Technical University of Gdańsk, Gdańsk, Poland. (in Polish).

Author biographies

Kandouci Chahr-Eddine, was born in 1960, received his Ph.D in 1992 from the Institute of Shipbuilding of Gdansk Technical University, and he is currently a senior lecturer at University of Sciences and Technology of Oran since 1992. His main research is dynamic of propelling systems.

Adjal Yassine, was born in 1982, received his Master degree from the University of Sciences and Technology of Oran-Algeria, currently he is Ph.D candidate, interested field focus on mechanical vibration.